

Fabrication and characterization of layer-by-layer nano self-assembled ZnO nanorods/carbon nanotube film sensor for ethanol gas sensing application at room temperature

Dongzhi Zhang¹  · Yan'e Sun¹ · Yong Zhang¹

Received: 22 May 2015 / Accepted: 19 June 2015 / Published online: 1 July 2015
© Springer Science+Business Media New York 2015

Abstract This paper reported a ZnO/multi-wall carbon nanotubes (MWNTs) film-based sensor for ethanol gas detection. The film sensor was fabricated on a printed circuit board with interdigital electrodes microstructure. ZnO and MWNTs were utilized to form a hierarchical nanostructure using layer-by-layer self-assembly technique. The ZnO/MWNTs nanocomposites were characterized by scanning electron microscope and X-ray diffraction. The ethanol gas sensing properties of the presented sensor, such as the sensitivity, response-recovery characteristics and repeatability, were investigated by exposing to different concentration of ethanol gas varying from 5 to 500 ppm at room temperature. Comparisons were made with the drop-casted ZnO and layer-by-layer self-assembled ZnO/PSS film sensors under the same design, substrate and experiment conditions. As a result, the ZnO/MWNTs film sensor exhibited outstanding sensitivity, prompt response-recovery time and good repeatability, which outstripped that of the other two sensors. Furthermore, the normalized response of the sensor as a function of ethanol gas concentration was shown in this work, and the possible sensing mechanism of the above mentioned sensor was discussed in detail. This work highlights the unique superiority of layer-by-layer self-assembled ZnO/MWNTs film for constructing ethanol gas sensors.

1 Introduction

Ethanol gas detection plays a significant role in many fields, including industrial monitoring, fuel processing, ethanol production, safety testing of food package, physiological research on alcoholism and societal applications [1, 2]. So far, many efforts have been made in seeking novel nanomaterial for enhancing gas-sensing properties, such as metal-oxide semiconductor materials including ZnO [3], SnO₂ [4] and Fe₂O₃ [5], carbon nanotubes (CNTs) [6] and polymer [7]. Among these nanomaterials, ZnO, as a typical *n* type semiconductor metal oxide [3, 8], has been widely investigated due to its unique properties, such as nano-size, stable physical and chemical properties. Up to now, ZnO materials have been successfully used as sensing materials for detecting ethanol, toluene and so on by converting the information in relation with gas type and concentration into electrical signals when exposed to different gases [9–11]. However, the gas sensors fabricated with pure ZnO have some drawbacks including low sensitivity, long response and recovery times and high operation temperature [12–14].

Carbon nanotubes have aroused tremendous attentions owing to their large surface area to volume ratio, high chemical inertness, nanoscale structure and hollow center, which make them suitable for current and future application in nanotechnology [15, 16]. A number of recent groups have reported the gas sensors based on multi-walled carbon nanotubes (MWNTs) due to their unique properties. Notably, recent advances demonstrated that the decoration of MWNTs with metal oxide nanoparticles or polymer was an alternative route for constructing high-performance gas sensors due to its high sensitivity, short response and recovery times and low cost. Liu et al. [17] reported an ethanol gas sensor using SnO₂/MWNTs as

✉ Dongzhi Zhang
dzzhang@upc.edu.cn

✉ Yong Zhang
paul_zhangyong@163.com

¹ College of Information and Control Engineering, China University of Petroleum (East China), Qingdao 266580, China

sensing materials at 300 °C, and exhibited improved ethanol sensing properties than that of pure SnO₂ in terms of the appropriate basal resistance and enhanced signal transfer brought by MWNTs. Parmar et al. [18] fabricated CuO/MWNT thin film based ethanol-sensors by dispersing CVD-prepared MWNTs in varying concentration over DC magnetron sputtered-CuO films, and the sensor exhibited enhanced sensing response at an operating temperature of 400 °C compared with bare CuO sample. Alizadeh et al. [19] prepared a chemiresistor sensor for the ethanol detection by mixing of MWNT as conducting element, nano-sized molecularly imprinted polymer as recognition element and poly(methyl methacrylate) as an adhesive substance.

An alternative cost-effective approach, a solution-based bottom-up assembly process called layer-by-layer (LbL) self-assembly, allowed for sequential adsorption of functional nanoparticles to form a hierarchical membrane [20–22]. The LbL assembly approach offers a promising way to yield ultrathin nanocomposite films. In this work, we demonstrated ethanol gas sensors based on LbL self-assembled ZnO/PSS and ZnO/MWNTs nanocomposite film. The sensor was fabricated on the substrate of printed circuit board (PCB) with interdigital electrodes (IDE). The ethanol gas sensing properties of pure ZnO, ZnO/PSS and ZnO/MWNTs were investigated at room temperature through exposing to different concentration of ethanol gas. As a result, it was found that the performance of ZnO/MWNTs film sensor towards ethanol gas outstripped that of the other two sensors. Finally, the possible sensing mechanism of the above mentioned sensors was discussed in detail.

2 Experiment

2.1 Experimental materials

The functionalized MWNTs with carboxylic acid groups were offered by Chengdu Organic Chemical Co. Ltd (Chengdu, China) with length of 10–30 μm and diameter of 20–30 nm were used in our experiment. Zn (NO₃)₂·6H₂O (>99 %) was supplied by Sinopharm Chemical Reagent Co. Ltd (Shanghai, China), and NaOH (>96 %) was supplied by West Long Chemical Limited by Share Ltd (Guangdong, China). Polyelectrolytes used for LbL assembly were 1.5 wt% poly (diallylimethylammonium chloride) [PDDA (Sigma-Aldrich Inc., USA), molecular weight (MW) of 200–350 K, polycation] and 0.3 wt% poly (sodium 4-styrenesulfonate) [PSS (Sigma-Aldrich Inc., USA), MW of 70 K, polyanion] with 0.5 M NaCl in both for enhancing the ionic strength and polyions adsorption.

2.2 Fabrication

The sensor was fabricated on a PCB substrate by using microfabrication technology. PCB as an electrical insulating material, such as plastic, is initially used for a sensor substrate owing to its lower cost than other existing substrates. A pair of Ni/Cu rectangular-ambulatory-plane interdigitated electrodes (RAP-IDEs) was deposited on PCB substrate via photolithographic technology. The IDEs pattern window on the PCB substrate has an outline dimension of 1 × 1 cm, the electrode thickness is 50 μm and the width and gap both is 200 μm.

The sensing film of ZnO/MWNTs was fabricated by the combination of hydrothermal synthesis and LbL nano self-assembly technique, as shown in Fig. 1. In the typical process, the first step was the preparation of ZnO nanoparticles by using a hydrothermal method. 2.08 g Zn (NO₃)₂·6H₂O was dissolved into 140 mL deionized (DI) water with stirring for 1 h, and 20 mL of NaOH (4 mol/L) was added into the resulting solution with stirring for 30 min. And then, the as-prepared solution was transferred into a 200 mL stainless-steel autoclave and heated at 120 °C for 12 h. Afterward, when the autoclave cooled down to room temperature, the final product of ZnO suspension was washed with DI water and anhydrous ethanol for several times to remove excess ions, and subsequent was ultrasonicated for 1 h and centrifugated for 15 min. The second step is the LbL self-assembly process for fabricating sensing film of ZnO/MWNTs. Two bi-layers of PDDA/PSS were firstly self-assembled as precursor layers for charge enhancement, and then three bi-layers of ZnO/MWNTs were performed by using LbL self-assembly technique. The immersing time here used was 10 min for polyelectrolytes and 15 min for ZnO and MWNTs, and intermediate rinsing with DI water and drying with nitrogen flow were required after each monolayer assembly to reinforce the interconnection between layers. Afterward, the self-assembled ZnO/MWNTs film devices are heated at 80 °C for 2 h. Finally, the sensor was dried in the oven at 50 °C for 2 h. The schematic diagram of ZnO/MWNTs nanocomposite sensor along with hierarchical structure was shown in the Fig. 2. The ZnO/PSS film sensor was prepared by the same manner, while PSS was used instead of MWNTs. For making comparison, the pure ZnO film sensor was prepared by drop-casting of hydrothermal synthesized ZnO solution.

2.3 Instrument and analysis

The surface morphology of as-prepared ZnO nanoparticles, MWNTs and ZnO/MWNTs films were examined with field emission scanning electron microscopy (FESEM, Hitachi S-4800). And their XRD analyses were performed with

Fig. 1 Fabrication illustration of ZnO/MWNTs film using the combination of hydrothermal synthesis and LbL self-assembly

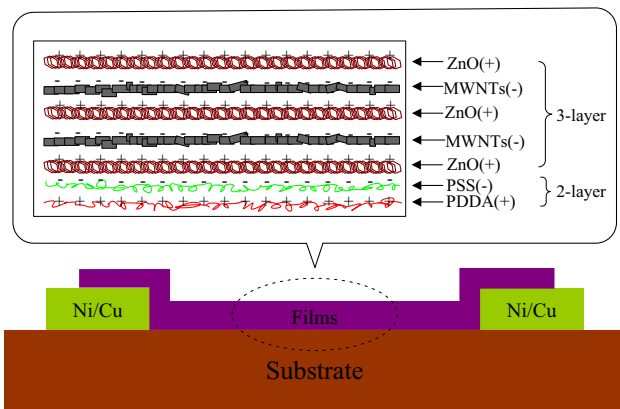
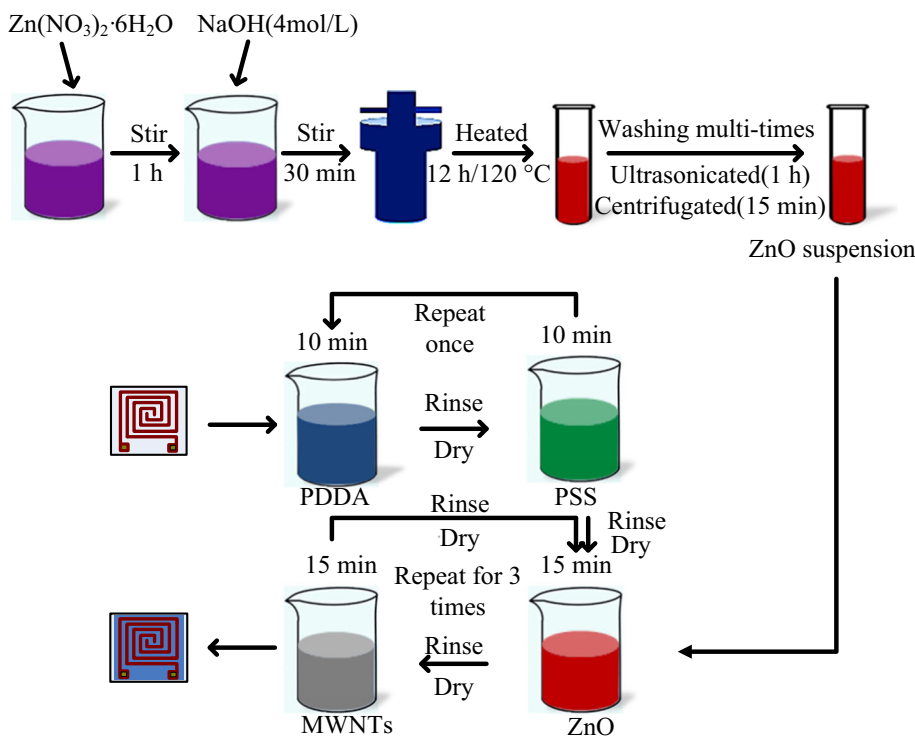


Fig. 2 Sketch of LbL self-assembled ZnO/MWNTs film sensor

X-ray diffractometer (Rigaku D/Max 2500PC, Japan) using Cu K α ($\lambda = 1.5418 \text{ \AA}$) radiation with a 2θ scanning range of 10° – 50° at room temperature.

The ethanol gas sensing experiment was performed at room temperature, and the response properties were measured using a data logger (Agilent 34970A). The gas sensing properties were investigated by exposing the gas sensors to various concentrations of ethanol gas varying from 5 to 500 ppm, and the desired gas concentration is obtained by injecting a required quantity of anhydrous liquid ethanol into a sealed glass container by using a syringe. The concentration of injected ethanol in the chamber was calculated in ppm is described as [23],

$$C = \frac{22.4\rho TV_s}{273MV} \times 1000 \tag{1}$$

where C is the concentration of gaseous ethanol (ppm), ρ is the density of liquid ethanol (g/mL), T is the testing temperature (K), V_s is the volume of liquid ethanol (μL), M is the molecular weight of ethanol (g/mol), and V is the volume of the chamber (L). In our work, the values of M , P , R , ρ and T are 46 g/mol, 101,325 Pa, 8.31441 J/(mol K), 0.789 g/cm 3 , 298 K, respectively.

The change of ethanol gas concentration was converted to the corresponding electrical resistance variation of the sensors. The figure of merit used to characterize the sensor performance is the normalized response (S), determined as $S = (R_a - R_g)/R_a \times 100\%$, where R_a and R_g were the sensor resistance in dry air and ethanol gas, respectively. The time taken by a sensor to achieve 90% of the total resistance change is defined as the response or recovery time.

3 Results and discussion

3.1 SEM and XRD characterization

Figure 3 shows the observed SEM and XRD results of ZnO nanoparticles, MWNTs and ZnO/MWNTs film. Figure 3a shows the as-prepared ZnO was nanorod-shaped crystal. Figure 3b indicates the interdigitated or interweaved

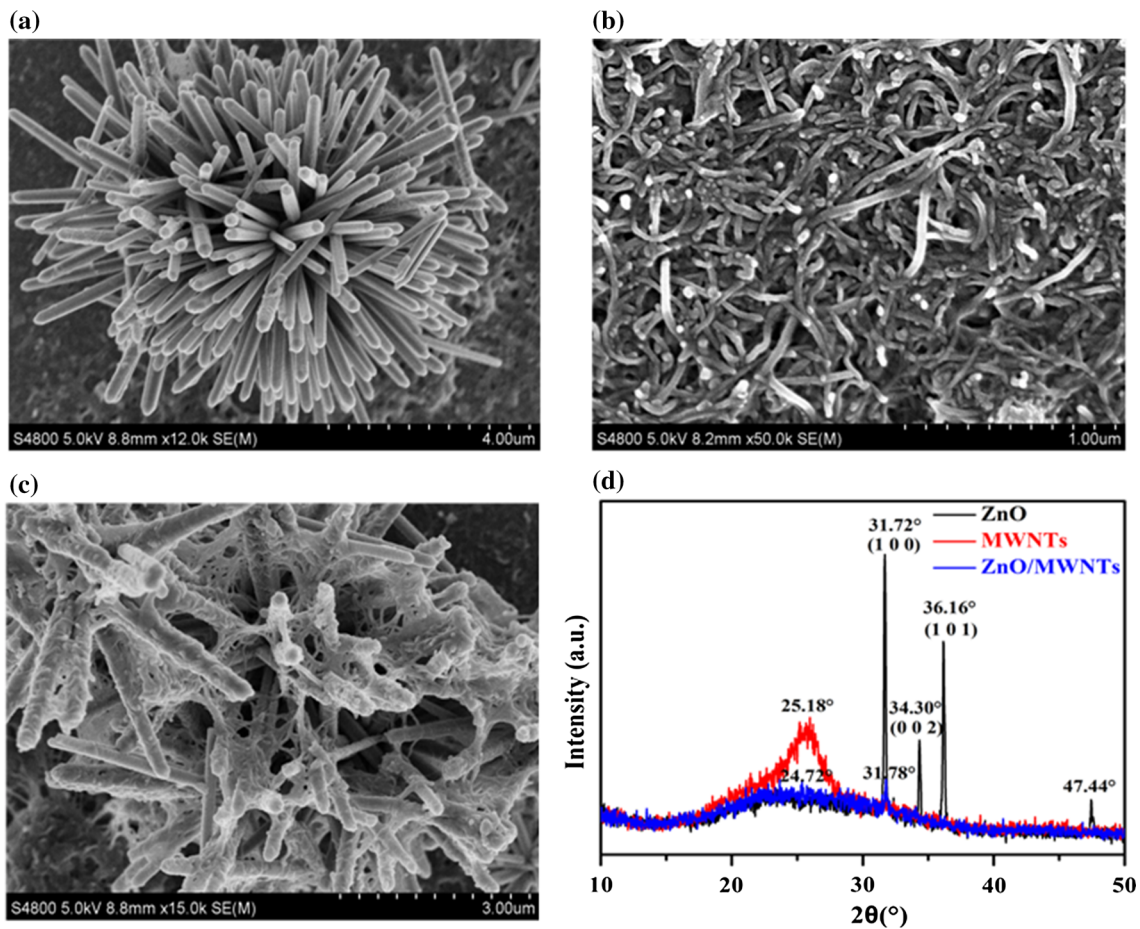


Fig. 3 SEM and XRD observation of ZnO, MWNTs, ZnO/MWNTs films

MWNTs with a random network structure. Figure 3c shows the ZnO/MWNTs film is constructed by ZnO nanorods and MWNTs wrapped closely together. Figure 3d plots the XRD spectrum for ZnO, MWNTs, ZnO/MWNTs film. XRD of the ZnO shows polycrystalline structure with major peaks at 31.72° , 34.30° and 36.16° , which were attributed to the diffracting planes (1 0 0), (0 0 2), (1 0 1) of ZnO nanocrystals. A peak at 2θ angle of 25.18° for MWNTs and major peaks at 2θ angle of 24.72° and 31.78° for ZnO/MWNTs nanocomposite were obviously observed in the XRD patterns of MWNTs and ZnO/MWNTs nanocomposite. The peaks attributed to the (0 0 2), (1 0 1) planes were not obvious in the XRD spectrum of ZnO/MWNTs, probably due to that the ZnO nanocrystallines was covered or wrapped by MWNTs.

3.2 Ethanol-sensing properties

Figure 4 shows the real-time resistance measurement of the ZnO/MWNTs film sensor exposed to various concentration of ethanol gas from 5 to 500 ppm. Each exposure/recovery cycle is performed by an exposure interval of 100 s under

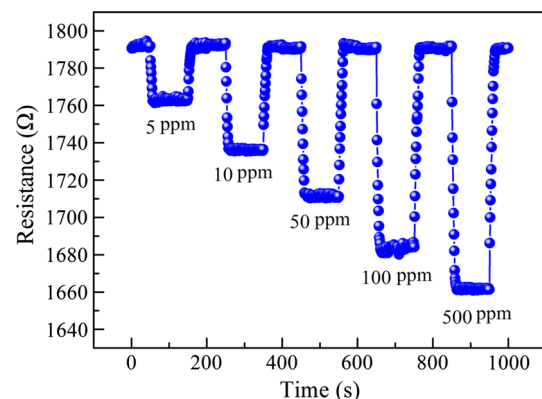


Fig. 4 Resistance measurement of the ZnO/MWNTs film sensor toward ethanol gas ranging from 5 to 500 ppm at room temperature

different ethanol concentration followed by a recovery interval of 100 s at dry air. A clear decrease in the sensor resistance is observed with the ascending ethanol concentration in range of 5–500 ppm, and the corresponding normalized response values are calculated to be 1.6, 3, 4.5, 5.9 and 7.3 % when the sensor exposed to 5, 10, 50, 100

and 500 ppm. The sensor exhibited a good sensing performance and ppm-level detection towards ethanol gas at room temperature.

The repeatability of ZnO/MWNTs nanocomposites sensor is measured for three exposure/recovery cycles repeatedly to ethanol gas concentration of 5, 10, 50 ppm under the same experimental conditions, and the measured results are shown in Fig. 5. The results in Fig. 5 show an outstanding response and recovery behavior and acceptable repeatability for the sensor. Figure 6 shows the response and recovery curve of the ZnO/MWNTs nanocomposites sensor under different ethanol concentration. The interval of gas-sensing film exposed to ethanol gas and dry air was selected to be 100 s. The response and recovery times are observed as 5–12 and 8–16 s, respectively.

In order to further investigate the advantages of the proposed sensor, the gas sensing properties of pure ZnO sensor, ZnO/PSS and ZnO/MWNTs sensors were compared in Fig. 7. ZnO sensor was fabricated with pure ZnO nanoparticles by drop-casting method, and ZnO/PSS nanocomposite sensor was fabricated with ZnO nanoparticles and PSS by LbL self-assembly method. The three sensors were tested under the same experimental environment with ethanol gas concentration ranging of 5–500 ppm. It is found that the sensing properties of the ZnO/MWNTs nanocomposite sensor were much better than that of pure ZnO sensor and ZnO/PSS nanocomposite sensor. For instance, the normalized response values are 2.6, 3 and 4.5 %, respectively, for pure ZnO, ZnO/PSS and ZnO/MWNTs sensors exposed to 50 ppm ethanol gas. Furthermore, Fig. 8 shows the comparison results in the response and recovery characteristics for the three sensors exposed to 50 ppm ethanol gas. The response time is 13, 11 and 7 s, and the recovery time is 17, 19 and 11 s for ZnO, ZnO/PSS and ZnO/MWNTs sensor, respectively. It is clear

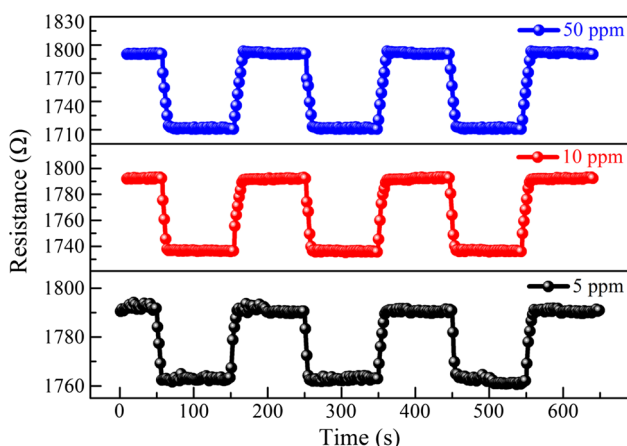


Fig. 5 The repeatability curve of the ZnO/MWNTs nanocomposites film sensor for ethanol gas of 5, 10, 50 ppm at room temperature

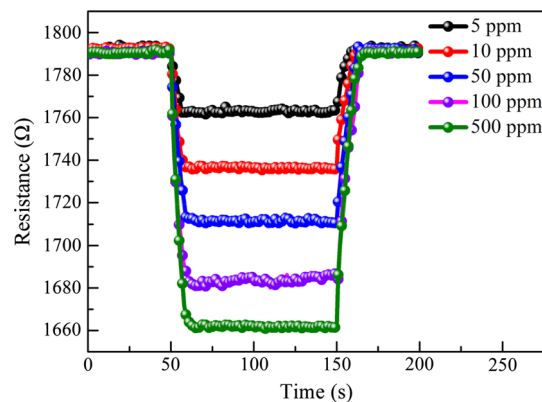


Fig. 6 The response and recovery curves of the ZnO/MWNTs film sensor toward ethanol concentrations ranging from 5 to 500 ppm

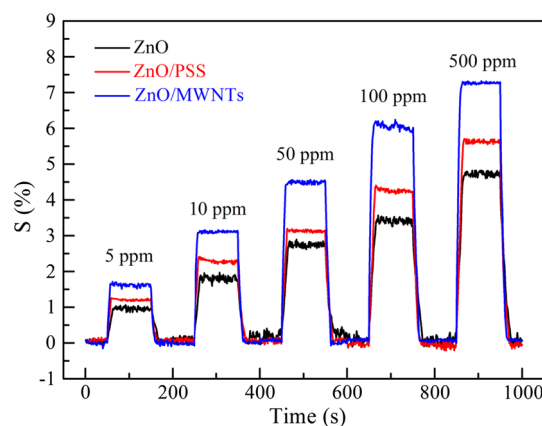


Fig. 7 Normalized response of ZnO, ZnO/PSS and ZnO/MWNTs film sensors exposed to various ethanol concentrations

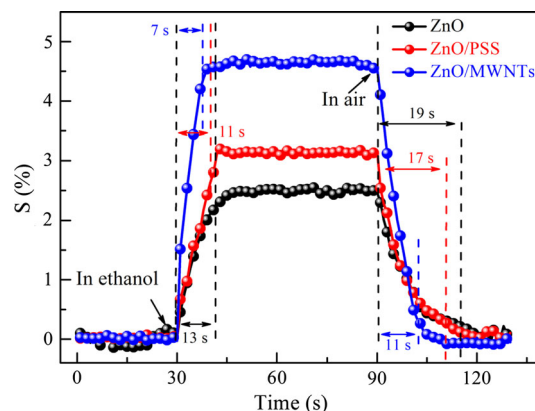


Fig. 8 The response and recovery characteristics of ZnO, ZnO/PSS, ZnO/MWNTs film sensors exposed to 50 ppm ethanol gas at room temperature

that the ZnO/MWNTs sensor has much shorter response and recovery time than that of the other two sensors.

Figure 9 shows normalize response of ZnO, ZnO/PSS, ZnO/MWNTs film sensor as a function of ethanol gas

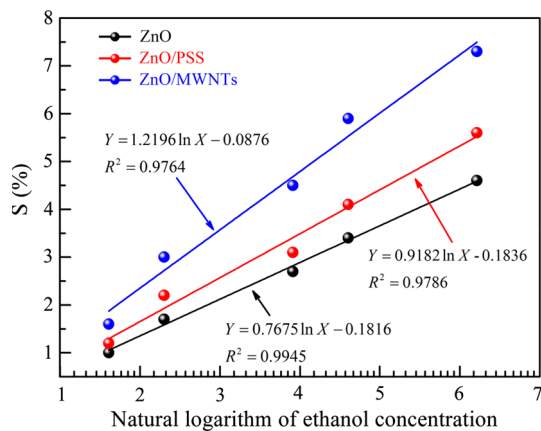


Fig. 9 Normalized response of ZnO, ZnO/PSS, ZnO/MWNTs film sensor as a function of ethanol gas concentration

concentration. The fitting equation for normalized response Y as a function of ethanol gas concentration X can be represented as $Y = 0.7675 \ln X - 0.1816$, $Y = 0.9182 \ln X - 0.1836$ and $Y = 1.1296 \ln X - 0.0876$ for the pure ZnO, ZnO/PSS and ZnO/MWNTs film sensor, respectively, and the fitting correlation coefficient, R^2 , is 0.9945, 0.9786 and 0.9764, respectively. It is found that the normalized response of the sensors exhibited a good linearity with the natural logarithm of ethanol gas concentration, and the ZnO/MWNTs film sensor demonstrated a highest sensitivity among the three sensors.

3.3 Gas-sensing mechanism

From the above mentioned experiments, we can find that ZnO/MWNTs film sensor is more sensitive to ethanol molecules than ZnO/PSS film and pure ZnO film. As we known, ZnO has some outstanding physicochemical properties, such as high surface-to-volume, good electrical conductivity [24, 25]. It is notable that ZnO/PSS film sensor has a higher performance than that of pure ZnO sensors, mainly attribute to the ZnO nanoparticles were uniformly dispersed in PSS matrix under the electrostatic interaction. Thereby a hybrid nano-structure was created and the agglomeration of ZnO nanoparticles was reduced. The high-performance of the ZnO/MWNTs film sensor can be attributed to three factors. Firstly, MWNTs have a large specific surface area owing to its special hollow tubular structure [26–28], and carboxylic acid functional groups attached on the nanotubes surface provide reactive sites for ethanol gas absorption and thus lead to electrons transfer between the surface and the internal, appearing as the change in the electrical resistance upon ethanol exposure. Second, the good electrical conductivity, metallicity and semiconducting property of MWNTs make the resistivity of ZnO/MWNTs nanocomposites film is far less than the pure ZnO and ZnO/PSS film under room temperature [29,

30]. Thirdly, p–n heterojunctions can be created at the interface between n type ZnO and p type MWNTs. The differences in the band-gap and Fermi level between the ZnO and the MWNTs are modified through band bending in the depletion layer when adsorbing or desorbing ethanol gas molecules. The adsorbed gas molecules at the p–n heterojunction lead to a decrease of the depletion layer, and subsequently result in a fall of sensor resistance.

4 Conclusions

In this paper, we fabricated a ZnO/MWNTs film sensor on the PCB substrate using Lbl self-assembly technique. The film structures were examined by scanning electron microscope (SEM) and X-ray diffraction (XRD). The ethanol gas sensing properties of the presented sensor were investigated by exposing to different concentration of ethanol gas at room temperature. Comparisons were made with the drop-casted ZnO and LbL self-assembled ZnO/PSS film sensors under the same design, substrate and experiment conditions. As a result, the ZnO/MWNTs film sensor exhibited outstanding sensitivity, prompt response-recovery time and good repeatability, which outstripped that of the other two sensors. Furthermore, the possible sensing mechanism of the above mentioned sensors was discussed in detail. This work highlights the unique superiority of LbL self-assembly for gas sensors fabrication.

Acknowledgments This work was supported by the National Natural Science Foundation of China (Grant No. 51407200), the Science and Technology Plan Project of Shandong Province (Grant No. 2014GSF117035), the Promotive Research Foundation for the Excellent Middle-Aged and Youth Scientists of Shandong Province of China (Grant No. BS2012DX044), the Science and Technology Development Plan Project of Qingdao (Grant No. 13-1-4-179-jch), the Open Fund of National Engineering Laboratory for Ultra High Voltage Engineering Technology (Kunming, Guangzhou) (Grant No. NEL201518), the Fundamental Research Funds for the Central Universities of China (Grant no. 15CX05041A), and the Science and Technology Project of Huangdao Zone, Qingdao, China (Grant No. 2014-1-51).

Compliance with Ethical Standards

Conflict of interest None.

References

1. A.L. Zou, L.Z. Hu, Y. Qiu, G.Y. Cao, J.J. Yu, L.N. Wang, H.Q. Zhang, B. Yin, L.L. Xu, High performance of 1-D ZnO micro-wire with curve-side hexagon as ethanol gas sensor. *J. Mater. Sci.: Mater. Electron.* (2015). doi:10.1007/s10854-015-3001-8
2. W. Tan, Q. Yu, X. Ruan, X. Huang, Design of SnO₂-based highly sensitive ethanol gas sensor based on quasi molecular-cluster imprinting mechanism. *Sens. Actuators, B* **212**, 47–54 (2015)

3. J.J. Qi, H. Zhang, S.N. Lu, X. Li, M.X. Xu, Y. Zhang, High performance indium-doped ZnO gas sensor. *J. Nanomater.* **2015**, 954747 (2015)
4. S. Liu, Y. Zhang, B. Yu, Z.Y. Wang, Solvent-free infiltration method to prepare mesoporous SnO₂ templated by SiO₂ nanoparticles for ethanol sensing. *Sens. Actuators, B* **210**, 700–705 (2015)
5. Y.L. Cao, H.Y. Luo, C. Wang, D.Z. Jia, Low-heating solid-state synthesis and excellent gas-sensing properties of α -Fe₂O₃ nanoparticles. *Sens. Actuators, B* **176**, 618–624 (2013)
6. N.V. Hieu, N.A.P. Duc, T. Trung, M.A. Tuan, N.D. Chien, Gas-sensing properties of tin oxide doped with metal oxides and carbon nanotubes: a competitive sensor for ethanol and liquid petroleum gas. *Sens. Actuators, B* **144**, 450–456 (2010)
7. D.Z. Zhang, K. Wang, J. Tong, B.K. Xia, Characterization of layer-by-layer nano self-assembled carbon nanotube/polymer film sensor for ethanol gas sensing properties. *Microsyst. Technol.* **20**, 379–385 (2014)
8. W. Tang, J. Wang, Mechanism for toluene detection of flower-like ZnO sensors prepared by hydrothermal approach: charge transfer. *Sens. Actuators, B* **207**, 66–73 (2015)
9. L.W. Wang, Y.F. Kang, Y. Wang, B.L. Zhu, CuO nanoparticle decorated ZnO nanorod sensor for low-temperature H₂S detection. *Mater. Sci. Eng., C* **32**, 2079–2085 (2012)
10. Q.Q. Jia, H.M. Ji, Y. Zhang, Y.L. Chen, X.H. Sun, Z.G. Jin, Rapid and selective detection of acetone using hierarchical ZnO gas sensor for hazardous odor markers application. *J. Hazard. Mater.* **276**, 262–270 (2014)
11. S. Liu, B. Yu, H. Zhang, T. Fei, T. Zhang, Enhancing NO₂ gas sensing performances at room temperature based on reduced graphene oxide-ZnO nanoparticles hybrids. *Sens. Actuators, B* **202**, 272–278 (2014)
12. K.H. Kim, Z.G. Jin, Y. Abe, M. Kawamura, A comparative study on the structural properties of ZnO and Ni-doped ZnO nanostructures. *Mater. Lett.* **149**, 8–11 (2015)
13. C.S. Chen, X.D. Xie, G.J. Zhao, B. Zeng, X.T. Ning, S.Y. Cao, Y. Xiao, Y.P. Mei, X.M. Huang, Graphene/multi-walled carbon nanotube composite as an effective supports to enhance the photocatalytic property of Cu-doped ZnO nanoparticles. *Funct. Mater. Lett.* **6**, 1350062 (2013)
14. S. Zhan, D.M. Li, S.F. Liang, X. Chen, X. Li, A novel flexible room temperature ethanol gas sensor based on SnO₂ doped polydiallyldimethylammonium chloride. *Sensors* **13**, 4378–4389 (2013)
15. M. Mazloum-Ardakani, A. Khoshroo, L. Hosseinzadeh, Simultaneous determination of hydrazine and hydroxylamine based on fullerene-functionalized carbon nanotubes/ionic liquid nanocomposite. *Sens. Actuators, B* **214**, 132–137 (2015)
16. P.C. Tsai, Y.R. Jeng, Effects of nanotube size and roof-layer coating on viscoelastic properties of hybrid diamond-like carbon and carbon nanotube composites. *Carbon* **86**, 163–173 (2015)
17. L. Liu, J. Zhuang, K.X. Liu, L.Y. Wang, S.C. Li, W. Li, X.L. Li, Improved and excellent ethanol sensing properties of SnO₂/multiwalled carbon nanotubes. *Chin. Sci. Bull.* **55**(4–5), 382–385 (2010)
18. M. Parmar, R. Bhatia, V. Prasad, K. Rajanna, Ethanol sensing using CuO/MWNT thin film. *Sens. Actuators, B* **158**, 229–234 (2011)
19. T. Alizadeh, F. Rezaloo, A new chemiresistor sensor based on a blend of carbon nanotube, nano-sized molecularly imprinted polymer and poly methyl methacrylate for the selective and sensitive determination of ethanol vapor. *Sens. Actuators, B* **176**, 28–37 (2013)
20. D. Zhang, J. Tong, B. Xia, Q. Xue, Ultrahigh performance humidity sensor based on layer-by-layer self-assembly of graphene oxide/polyelectrolyte nanocomposite film. *Sens. Actuators, B* **203**, 263–270 (2014)
21. D. Zhang, T. Cui, Tunable mechanical properties of layer-by-layer self-assembled carbon nanotube/polymer nanocomposite membranes for M/NEMS. *Sens. Actuators A Phys.* **185**, 101–108 (2012)
22. D. Zhang, J. Tong, B. Xia, Humidity-sensing properties of chemically reduced graphene oxide/polymer nanocomposite film sensor based on layer-by-layer nano self-assembly. *Sens. Actuators, B* **197**, 66–72 (2014)
23. D. Zhang, A. Liu, H. Chang, B. Xia, Room-temperature high-performance acetone gas sensor based on hydrothermal synthesized SnO₂-reduced graphene oxide hybrid composite. *RSC Adv.* **5**, 3016–3022 (2015)
24. C.J. Shao, Y.Q. Chang, Y. Long, High performance of nanostructured ZnO film gas sensor at room temperature. *Sens. Actuators, B* **204**, 666–672 (2014)
25. Z.H. Khan, N.A. Salah, S.S. Habib, A. Azam, M.S. El-Shahawi, Multi-walled carbon nanotubes film sensor for carbon mono-oxide gas. *Curr. Nanosci.* **8**, 274–279 (2012)
26. R. Arsat, X. He, R. Spizzirri, M. Shafiei, M. Arsat, W. Wlodarski, Hydrogen gas sensor based on highly ordered polyaniline/multi-wall carbon nanotubes composite. *Sens. Lett.* **9**, 940–943 (2011)
27. J.M. Wu, A room temperature ethanol sensor made from p-type Sb-doped SnO₂ nanowires. *Nanotechnology* **21**, 235501 (2010)
28. Y.F. Li, L.N. Zou, Y. Li, K.J. Li, B.X. Ye, A new voltammetric sensor for morphine detection based on electrochemically reduced MWNTs-doped graphene oxide composite film. *Sens. Actuators, B* **201**, 511–519 (2014)
29. W.C. Wang, Y.T. Tian, X.C. Wang, H. He, Y.R. Xu, C. He, X.J. Li, Ethanol sensing properties of porous ZnO spheres via hydrothermal route. *J. Mater. Sci.* **48**, 3232–3238 (2013)
30. A. Bejaoui, J. Guerin, K. Aguir, Modeling of p-type resistive gas sensor in the presence of a reducing gas. *Sens. Actuators, B* **181**, 340–347 (2013)